Performance Comparison of Various Nonlinear Control Strategies Applied to ESC

K. Chatrath (4739205), N. Chowdhri (4744055),
M. Damian (4749705), P. Vitiello (4719557)
M. Mechanical Engineering, Delft University of Technology, Delft, The Netherlands

***Abstract*—An ESC system improves the stability of a vehicle when it operates in extreme manoeuvres or operates close to the limits of handling. It involves control of the vehicle's yaw rate and body slip angle, typically by differential braking. An ESC system has two levels of control, namely high and low level. ESC systems, in recent years, have gained popularity in the market and are proving to be effective in improving safety, comfort and handling. However, stability related fatal accidents are still reported despite vehicles being equipped with ESC. The following study attempts to formulate alternate and effective high level control strategies. This has been tested using MATLAB and Simulink and the controllers are validated on a nonlinear multibody vehicle model. Typically, controllers apply a corrective action on the yaw rate of the vehicle. In this report, three nonlinear high level controllers are formulated and tested (by simulation) as the vehicle undergoes specific manoeuvres, in order to assess and compare performance. The study shows a transition from simple yaw rate control to an observer based integrated control strategy. The integrated control strategy involves generation of a corrective action on yaw rate as well as lateral velocity. This ensures better ride handling, safety and comfort.**

I. Introduction

As technology progresses, the need for precise and effective control increases as well; this principle is already acted upon in all innovative technologies centered around human well being. Keeping this in mind, the Automotive Society incessantly deploys its energies to improve overall driving stability and passengers' safety. The first noteworthy achievement was represented by the development of Antilock Braking System (early 1928); however, since the early stages this system has undergone many refinements to achieve an acceptable level of safety and become commercially available.

With the passing of time, technological developments have allowed us to further extend the use of control theory on vehicle dynamics, and an increasing number of unsolved problems were approached and tackled: among these the most important and widely recognized problems is the lack of stability control.

A typical scenario in which such problem occurs depicts the driver travelling at high-speed and suddenly an obstacle appears on his path: in such situations the driver will be forced to take a sharp turn or apply brakes to avoid a possible collision; while doing so, he might lose control and skid off the road. To avoid the occurrence of such undesired vehicle behaviour, car manufacturers employ on modern cars an Electronic Stability Control (**ESC**) as active safety systems. A picture of the depicted scenario is provided in Fig. 1 for explanatory purposes.

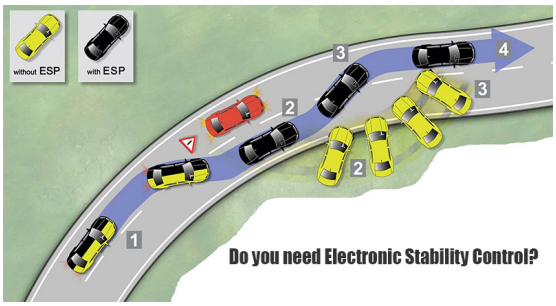

Fig. 1. An Emergency Scenario showing the effectiveness of the ESC [1].

The ESC in particular will intervene when sensors detect that a driver is approaching a predetermined stability limit, that could result in the vehicle taking a path other than the intended one. As previously anticipated, the ESC deals with the control of the lateral dynamics in those situations in which the external excitation become so high to induce a nonlinear behaviour in the tire response, i.e. force generations. Under this perspective, the main purpose of the ESC is to reduce as much as possible the permanence of the vehicle in the limit handling regions, indicated in red in Fig. 2.

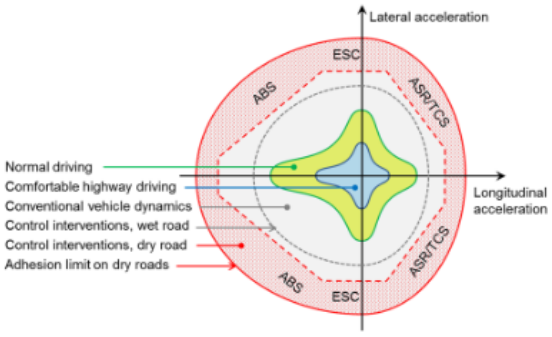

Fig. 2. Vehicle Handling Regions per acceleration values - *Daimler*.

As a matter of fact, since the introduction of this technology at a commercial level, the driving safety of the passenger cars has increased steadily. In particular NHTSA confirms with its statistic studies that from 2011, over a 5 years period, the number of lives saved in the US, because of ESC implementation, has more than doubled [2].

Even though statistics show improvements, the same studies demonstrate that, despite ESC implementation, 2,272 fatalities over the same period occurred despite of the ESC presence. This particular detail represents the motivation at the basis

of this paper, which main aim is to investigate the fallacy of the classical control implementation and show that, by means of nonlinear approach, better results can be achieved, both from comfort, performance and safety perspective. Developing a gradual digression, the applied control strategy will first acquire the shape of a nonlinear state feedback strategy, namely *Lyapunov Approach*, to progressively increase in complexity, first with the implementation of a *Super Twisting Algorithm*, to finally come up with a more general approach, assuming a more realistic set of reduced available signals and an additional vehicle parameter to be controlled, to eventually establish an integrated control strategy through an *Observer-based Adaptive Super Twisting Algorithm*.

The three cited controllers are then validated on a *Non-linear Multibody Vehicle Model* performing different driving manoeuvres, in order to better capture and compare their effectiveness from different perspectives.

II. Control Strategies

In this section the implemented control strategies will be examined in increasing order of complexity and the required stability criteria will be either defined or addressed in the reference papers.

A. Non Linear State Feedback

The first control strategy involves the design of a non linear state feedback based on a Lyapunov analysis. The control design is a model based approach. The controller is based on a simple 2-DOF nonlinear vehicle model, indicated in Eq. 1.

$$\begin{aligned} P &= \frac{1}{M}((F_{yfl}+F_{yfr})\cos(\delta)+(F_{yrl}+F_{yrr})) \\ Q &= l_f(F_{yfl}+F_{yfr})\cos(\delta)-l_r(F_{yrl}+F_{yrr}) \\ &+ h_{tf}(F_{yfl}-F_{yfr})\sin(\delta) \\ \dot{v} &= P-ur \\ \dot{r} &= \frac{1}{I_z}(Q+M_z) \end{aligned} \tag{1}$$

It is assumed here that the measurements available for control design are those of lateral acceleration a_y, yaw rate r, longitudinal velocity v_x and lateral velocity v_y.

M_z represents the corrective yaw moment that is applied by the controller. To derive the controller, the following candidate Lyapunov function is considered:

$$V = \frac{A(v-v_{ref})^2}{2} + \frac{BI_z(r-r_{ref})^2}{2} \tag{2}$$

The above candidate function is positive definite. A and B are positive real tuning parameters

$$\dot{V} = A(v-v_{ref})\dot{v} + B(r-r_{ref})I_z\dot{r} \tag{3}$$

Replacing expressions for $\dot{v}$ and $\dot{r}$, we get the following. It is to be noted that $v_{ref}=0$

$$\dot{V} = Av(P-ur) + B(r-r_{ref})(Q+M_z) \tag{4}$$

In order to ensure that the time derivative of the Lyapunov function candidate is negative semi definite, the expression for corrective moment is chosen as

$$M_z = \frac{-Av(P-ur)}{B(r-r_{ref})} - Q - K(r-r_{ref}) \tag{5}$$

Here K is a positive tuning gain. Finally, the resulting expression for $\dot{V}$ is

$$\dot{V} = -BK(r-r_{ref})^2 \tag{6}$$

The time derivative is negative semi definite. In order to establish asymptotic stability, LaSalle's invariance principle can be invoked. One can observe that as the yaw rate approaches the reference yaw rate, the control action can become badly scaled and cause further numerical issues. In order to avoid such an eventuality, a minor modification is made to the control action equation which finally reads.

$$M_z = \frac{-Av(P-ur)}{B(r-r_{ref}+\epsilon)} - Q - K(r-r_{ref}) \tag{7}$$

The parameter ϵ is a small positive number which ensures that the denominator does not approach zero under any circumstances.

B. Second order sliding mode control with super twisting algorithm [3]

Sliding Mode Control (SMC) is a nonlinear state-feedback control scheme in which a discontinuous control action forces the system to switch from one continuous phase space to other by sliding the system's trajectory across the sliding surface.

SMC is an efficient method for parameter variation and accurate reference tracking. But the conventional SMC is not extensively used in practice. The discontinuous control action switches rapidly due to the excitation of unmodeled dynamics, leading to a high frequency phenomenon called 'chattering'-finite frequency and undesired finite amplitude oscillations [4].

To attenuate this effect, Higher Order SMC (HOSMC) like Second Order SMC (SOSMC) is implemented on the second derivative of the sliding surface to ensure that the sliding surface and its derivative go to zero in finite time. Use of SOSMC still guarantees robustness and accuracy.

But, it is very difficult to get the information on the sliding surface up to the second time derivative. To solve this problem, a modified SOSMC method called Super-twisting control law (STW) is used which does not require the time derivatives of the sliding surface [5]. It works for a relative degree of 1 of the sliding surface.

STW generates a continuous control action that drives the sliding surface and its first time derivative to zero against unmodeled dynamics. The control law consists of 2 terms, the first one is defined as a discontinuous time derivative control action that drives the sliding surface to zero, and a continuous control action that avoids chattering [3]. Since the control action has a discontinuous term under the integral, chattering is not completely eliminated but attenuated [6].

It is assumed here that the measurements available for control design are those of v_x, v_y, a_x and r . This too, is a nonlinear bicycle model based controller.

To design SMC, first a sliding surface is chosen such that the system trajectories are driven to it when the control action is applied. This ensures that the closed loop dynamics are based on the equation of sliding surface. To have lateral stability, the sliding entity σ is defined as the error term between the yaw rate and the desired yaw rate.

$$\sigma = r - r_{ref} \tag{8}$$

The aim of the controller is to drive this error to zero. Thus, the sliding surface is defined as

$$\sigma = 0 \tag{9}$$

The first 2 derivatives of the SOSMC are defined as

$$\dot{\sigma} = \frac{1}{I_z}(l_f(F_{yfl} + F_{yfr}) - l_r(F_{yrl} + F_{yrr}) + M_z) - \dot{r}_{ref}$$
$$\ddot{\sigma} = \frac{1}{I_z}(l_f(\dot{F}_{yfl} + \dot{F}_{yfr}) - l_r(\dot{F}_{yrl} + \dot{F}_{yrr}) + \dot{M}_z) - \ddot{r}_{ref} \tag{10}$$

We define:

$$\dot{u} = \dot{M}_z \tag{11}$$

Now the aim of the control action should be to drive the system dynamics to the sliding surface in a finite time. From Eq.10, we see that the first derivative of the sliding surface depends on the control action M_z. Thus the relative degree of σ w.r.t. to control action is 1 which allows the control action to control and drive $\dot{\sigma}$ to zero, thus smoothing out the sliding surface and attenuate the chattering.
The control law is defined as summation of two control signals as defined below.

$$u_{st} = u_1 + u_2 \tag{12}$$

Where u_1 and u_2 obey the following equations:

$$\dot{u}_1 = \begin{cases} -u & |u| > 0 \\ -W sign(\sigma) & |u| \leq 0 \end{cases}$$

$$u_2 = \begin{cases} -\eta|\sigma_0|^p sign(\sigma) & |\sigma| > \sigma_0 \\ -\eta|\sigma|^p sign(\sigma) & |\sigma| \leq \sigma_0 \end{cases}$$

Here, u_1 is the integral of the discontinuous action and u_2 is the control action that avoids chattering. Finally, the control action that is fed in to correct the yaw moment of the car is:

$$M_z = -(l_f(F_{yfl} + F_{yfr}) + l_r(F_{yrl} + F_{yrr})) + I_z\dot{r}_{ref} + u_{st} \tag{13}$$

C. Observer-based Adaptive Super Twisting Algorithm [7]

1) Higher order sliding mode observer: To enhance the vehicle performance, ride comfort and safety of the passengers, the cars nowadays are equipped with lot of sensors and electrical control units to gather vehicle data, analyze it and perform the required corrective action. This brings redundancy, but it significantly increases the price of the vehicle. Moreover, often independent control strategies are implemented and this warrants the need for very sound activation logic, thereby raising the complexity of the controller. This creates a need to implement an integrated control scheme. In addition to that, a major part of vehicle accidents reported, are due to skidding, where the driver loses the control of car due to loss of tractive contact of tire with road. To ensure that the car still remains in control, one needs to design controllers not only for yaw rate but also for other dynamical parameters. In this case, to avoid skidding, the most important parameter to be controlled is the body slip angle β of the car. So far, the above 2 control strategies only accounts for control of yaw rate. Therefore, this third control strategy warrants the use of an integrated control scheme.

The method presents a control scheme where 2 corrective control actions are being imparted to r and β. But in reality, it is very difficult to calculate β. The definition for body slip angle is

$$\beta = tan^{-1}(\frac{v_y}{v_x}) \tag{14}$$

Eq.14 shows direct relationship between β and v_y. By using small angle approximation, Eq.14 can be written as

$$\beta \approx \frac{v_y}{v_x} \tag{15}$$

The measurement for v_x is available. Eq.15 implies that in order to control body slip angle, lateral velocity v_y needs to be controlled. By providing corrective steering wheel angle δ_c to the tire generated from an Active Front Steering (AFS) system, the lateral forces generated can be varied which in turn will vary a_y and v_y of the car. Thus β can be controlled. But practically it is very difficult to measure v_y and thus the control action δ_c cannot be calculated.

To solve this issue, an observer can be designed that can estimate based on system dynamic equations the value of v_y, namely $\hat{v}_y$. In this method, a HOSMC observer is designed to estimate v_y. To capture the behaviour of the car efficiently, the roll dynamics of the car has also been taken into consideration while estimating the lateral velocity. The observer equations are shown below.

$$\begin{aligned} \dot{\hat{v}}_x &= \hat{v}_y r + a_x - \frac{m_s}{m} hr\dot{\hat{\theta}} + v_1 \\ \dot{\hat{v}}_y &= -v_x r + \frac{J_x}{J_{x,e}} a_y - \frac{k_{x,e}}{J_{x,s}}\hat{\theta} - \frac{b_x}{J_{x,s}}\dot{\hat{\theta}} + v_2 \\ \ddot{\hat{\theta}} &= -\frac{k_{x,e}}{J_{x,e}}\hat{\theta} - \frac{b_x}{J_{x,e}}\dot{\hat{\theta}} + \frac{m_s}{J_{x,e}} h a_y \end{aligned} \tag{16}$$

Here v_1 and v_2 are the 2 sliding surfaces which depend on the longitudinal velocity error. They are defined as

$$\begin{aligned} v_1 &= k_1|\tilde{v}_x|^{\frac{1}{2}} sign(\tilde{v}_x) \\ v_2 &= k_2 sign(\tilde{v}_x) sign(r) \end{aligned} \tag{17}$$

Where $\tilde{v}_x$ is the error defined by the equation

$$\tilde{v}_x = v_x - \hat{v}_x \tag{18}$$

2) HOSMC super-twisting algorithm with adaptive gains: Now that $\hat{v}_y$ is available, the control action is derived. First being a HOSMC scheme, 2 sliding surfaces s_1 and s_2 are defined as the error terms for lateral velocity and yaw rate, the two being the main integral control components to achieve lateral stability.

$$\begin{aligned} s_1 &= \hat{v}_y - v_{y,ref} \\ s_2 &= r - r_{ref} \end{aligned} \tag{19}$$

The first time derivative of the sliding surfaces are-

$$\begin{aligned} \dot{s_1} &= \Delta F_{y,f}\left(\frac{J_x}{J_{x,e}}\frac{\mu_y}{m}\right) + \rho_1 + v_2 \\ \dot{s_2} &= \frac{1}{I_z}M_z + \rho_2 \end{aligned} \tag{20}$$

In Eq.20 that the time derivatives of s_1 and s_2 depends on the 2 control actions $\Delta F_{y,f}$ and M_z respectively. Thus it can be seen that the relative degree here for both the surfaces is 1 which is the entire basis of STW to avoid chattering as explained before. Here,

$$\Delta F_{y,f} = F_{y,f} - F_{y,f,d} \tag{21}$$

Eq.21, defined as the difference between the desired lateral forces and the lateral forces generated due to the steering wheel angle input applied by the driver, describes the corrective lateral forces that needs to be given to the car.
Referring to [7], the values of ρ_1 and ρ_2 were calculated. After equation manipulations, the expressions for $\dot{s}_1$ and $\dot{s}_2$ were defined as:

$$\begin{aligned} \dot{s}_1 &= -\lambda_{11}|s_1|^{\frac{1}{2}}sign(s_1) + \sigma_1 + \rho_1 \\ \dot{\sigma}_1 &= -\lambda_{12}sign(s_1) \end{aligned} \tag{22}$$

$$\begin{aligned} \dot{s}_2 &= -\lambda_{21}|s_2|^{\frac{1}{2}}sign(s_2) + \sigma_2 + \rho_2 \\ \dot{\sigma}_2 &= -\lambda_{22}sign(s_2) \end{aligned} \tag{23}$$

where λ_{11}, λ_{12}, λ_{21} and λ_{22} are the adaptive tuning parameters.

These manipulations led to the following equations for control actions,

$$\begin{aligned} \Delta F_{y,f} &= \frac{J_{x,e}}{J_x}\frac{m}{\mu_y}(\lambda_{11}|s_1|^{\frac{1}{2}}sign(s_1) + \sigma_1 - v_2) \\ M_z &= I_z(-\lambda_{21}|s_2|^{\frac{1}{2}}sign(s_2) + \sigma_2) \end{aligned} \tag{24}$$

It was mentioned previously that the actual correction given is the AFS angle δ_c that controls the body slip angle by varying the lateral velocity v_y of the car. To derive this, first we needed $\hat{v}_y$ to get $\Delta F_{y,f}$. Now, by using the inverse of the approximated Magic formula, we express the change in lateral forces in terms of the corrective action δ_c on the wheels as shown in Eq.25

$$\begin{aligned} \Delta F_{y,f}^{-1} &= \frac{1}{B_{y,f}}\tan\left[\left(\frac{1}{c_{y,f}}\right)\arcsin\left(\frac{\Delta F_{y,f}}{D_{y,f}}\right)\right] \\ \delta_c &= \Delta F_{y,f}^{-1} \end{aligned} \tag{25}$$

Being an integrated control strategy, the second control action calculated is the yaw moment correction M_z to correct the yaw rate of the car which we know is the primary aim of ESC.

At last, the only task left is to come up with the values of the tuning parameters $\lambda's$. Since the system parameters are dynamic in nature, it is very difficult to perform gain scheduling and come up with set of values for the gains that will perform at any speed, and road condition. Instead, in this approach the gains are calculated adaptively. By taking into account the system dynamics, the gains are calculated online which not only ensure that the controller works efficiently but is also robust to parameter variations of the system.

Using the adaptive law, the λ terms are governed by the equations

$$\dot{\lambda}_{11} = \begin{cases} \omega_1\sqrt{\frac{\gamma_1}{2}} & s_1 \neq 0 \\ 0 & otherwise \end{cases}$$

$$\lambda_{12} = 2\epsilon_1\lambda_{11} + \eta_1 + 4\epsilon_1^2 \tag{26}$$

$$\dot{\lambda}_{21} = \begin{cases} \omega_2\sqrt{\frac{\gamma_2}{2}} & s_2 \neq 0 \\ 0 & otherwise \end{cases}$$

$$\lambda_{22} = 2\epsilon_2\lambda_{21} + \eta_2 + 4\epsilon_2^2 \tag{27}$$

where ω_1, ω_2, γ_1, γ_2, η_1, η_2, ϵ_1 and ϵ_2 are user defined positive constants.

III. Controller and Vehicle Performance Assessment in Closed Loop

Having discussed the design of three controllers, the following step was testing and tuning of the controllers on the nonlinear multibody vehicle model. The manoeuvre chosen for controller tuning testing is *Sine with Dwell*.

A. Controller Performance - Sine with Dwell

The Sine with Dwell test is a standard manoeuvre that a vehicle is subjected to, to assess dynamics stability. Here, the initial longitudinal speed of the vehicle is 25m/s in all simulations. One must recall that the integrated control strategy involves the design of a nonlinear observer which is used to estimate the lateral velocity. The quality of assessment can be studied in Fig. 3.

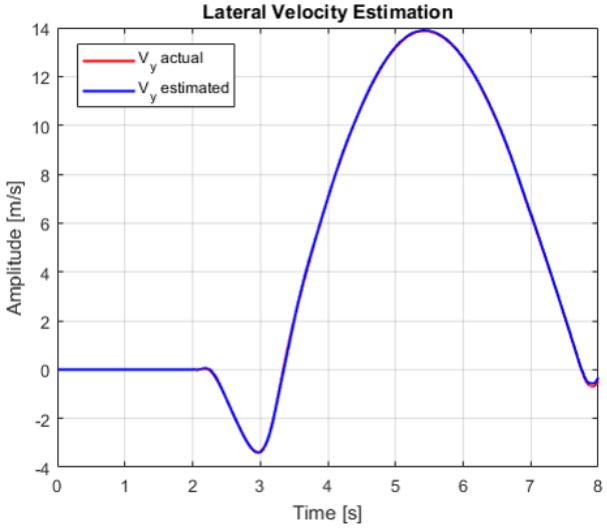

Fig. 3. Estimated Lateral velocity by the HOSM observer

It can be seen that the estimation is accurate. Having established the effectiveness of the HOSM observer, the results of the yaw rate responses for the tuned controllers is presented in Fig. 4. It can be seen that each of the controllers are able to let the vehicle track the reference yaw rate, that is quantified by

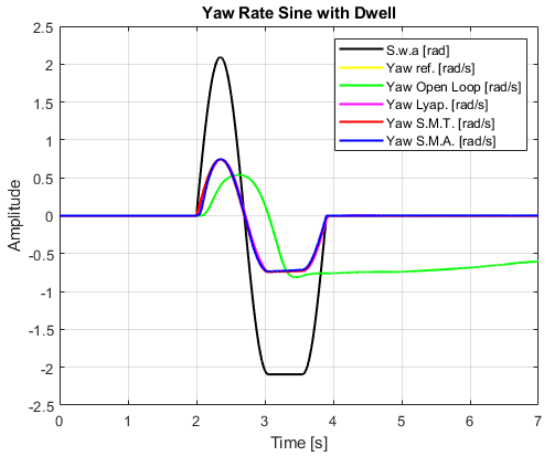

Fig. 4. Yaw rate vs. time - Sine with dwell manoeuvre

the steady state yaw rate gain, expressed in Eq. 28, multiplied by the steering input δ.

$$G_{yaw} = \frac{u}{L + K_{us}u^2} \tag{28}$$

with the understeer gradient defined as $K_{us} = \frac{ml_r}{LC_{\alpha_f}} - \frac{ml_f}{LC_{\alpha_r}}$ Fig. 5 shows the lateral displacement traversed by the vehicle in the aforementioned manoeuvre. It can be observed that all three controllers satisfy the evaluation criteria. The controllers ensure that the lateral displacement of the car is more than $1.83m$ at time $1.07s$ after the start of the manoeuvre. This ensures safety of the car. Also we can see from Fig. 5 that in open loop, the car crashes the evaluation criteria barrier and then goes out of control based on the trajectory observed. But with controllers, not only the barrier crash is avoided, the trajectories indicate that the vehicle is in control and has not gone out of the lane. In addition, it has to be pointed out that a remarkable result is obtained by the Integrated Approach controller, since the implementation of *AFS* allows to achieve a safe distance from the obstacle in the critical point and the narrowest cornering radius at the end of the manoeuvre. This ensures that the vehicle can close the corner better, reducing the offset from the ideal path.

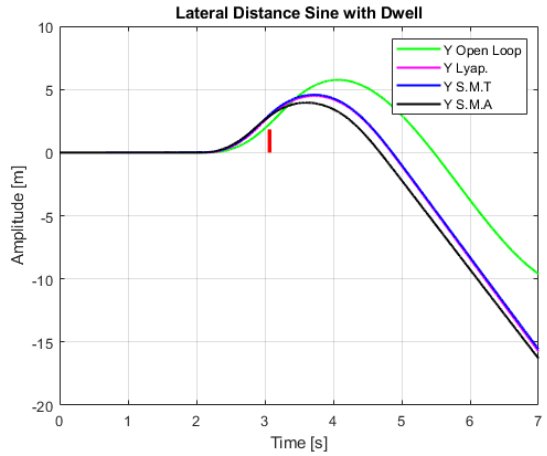

Fig. 5. Y displacement vs. time - Sine with dwell manoeuvre

The lateral velocity response can be studied in Fig. 6.

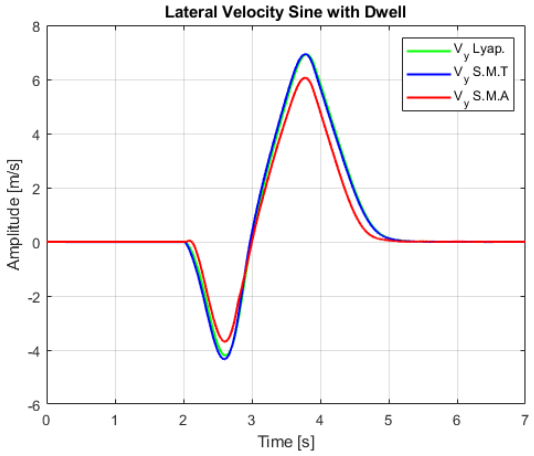

Fig. 6. Lateral velocity vs. time - Sine with dwell manoeuvre

From the lateral velocity response, it can be concluded that the integrated control scheme successfully reduces lateral velocity by almost 16.67% which in turn reduces body slip angle β.

B. Vehicle performance assessment - Step steer input

Having established the effectiveness of the controllers, the following step was to assess the vehicle performance in closed loop. To assess performance, one of the ways to do so is by the application of a step steer input. The input comprises of a step steering angle of 90^o counter clockwise. The lateral acceleration response can be assessed in Fig 7.

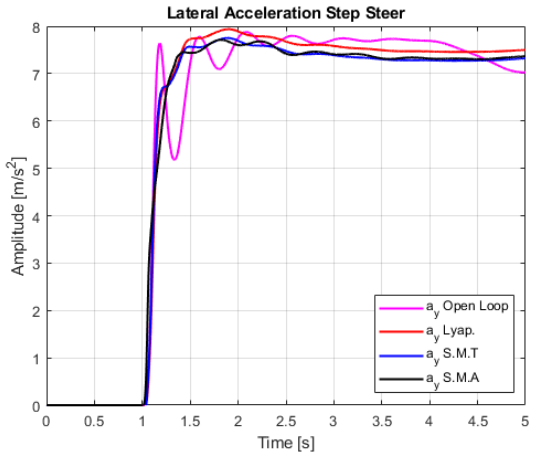

Fig. 7. Lateral acceleration vs. time - Step steer manoeuvre

It can be seen that the controllers reduce the oscillatory behaviour of the lateral acceleration response. This implies reduction in lateral jerk which in turn implies improved ride comfort. Moreover, the simple nonlinear state feedback controlled system shows highest lateral acceleration, thus implying better ride handling.

C. Vehicle performance assessment - Skidpad testing

The controllers were subjected to a second test namely skidpad test. There are three different testing protocols specified by [8], it was here chosen the one with a constant steering wheel angle. This was set equal to 45^o and the velocity was progressively increased from 15 m/s up to 25.21 m/s. To ensure that the steering wheel input remains constant for all control strategies, the AFS was deactivated in this manoeuvre. Therefore the integrated control law was merely reduced to a direct adaptive yaw moment correction.

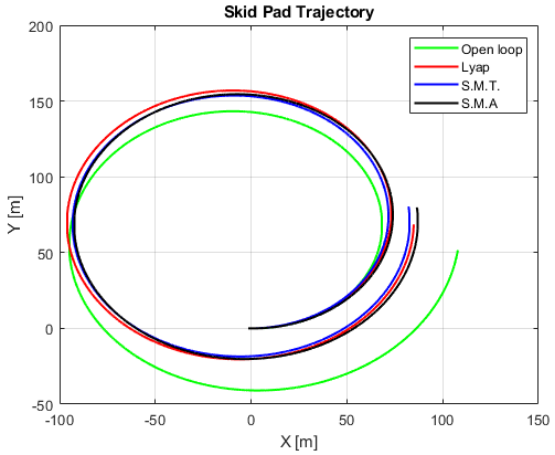

Fig. 8. Vehicle trajectories for a skidpad manoeuvre

Fig. 8 indicates that the vehicle tends to skid in open loop with an approximate radius of 110 m at the end of simulation. This skidding has been mitigated with the introduction of controllers; indeed the end time cornering radius is reduced to around 80 m. The skid in open loop is a result of high lateral velocity. It can be seen that the controllers enable the car to traverse around a smaller radius of curvature at higher longitudinal speeds. Furthermore, the traversal in closed loop takes place faster as the vehicle is ahead in closed loop as compared to open loop at the end of the manoeuvre. In order to compare the controllers, Fig 9 shows the lateral acceleration vs. time.

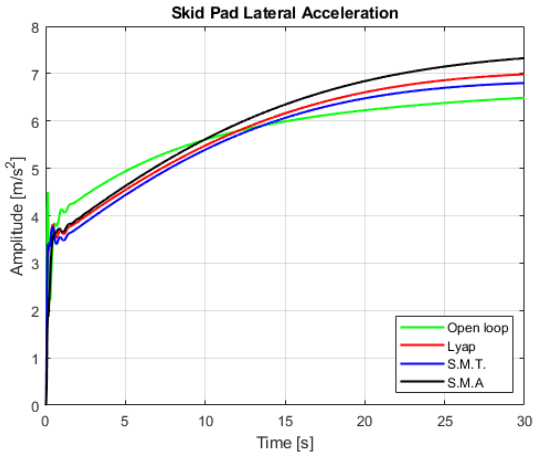

Fig. 9. Lateral acceleration vs. time - Skidpad manoeuvre

It can be seen that the observer based control strategy improves the vehicle's ride handling capabilities. The maximum lateral acceleration achievable is $7.4m/s^2$ which is an improvement of 15.6% w.r.t. open loop performance. The plot is similar to a step response. Also, it can be seen that observer based controller reduces initial over shoot which physically implies that the ride comfort has improved. In conclusion, the observer based controller enables the vehicle to traverse around a corner, faster.

D. Vehicle performance assessment - Sine with Dwell with mu split

To better appreciate the effectiveness of an integrated approach, a modified version of the Sine with Dwell has been performed; in particular, while performing the steering dwell a μ-split condition is imposed on the vehicle, critically decreasing the friction coefficient to 0.1 on the outer wheels to induce a counterclockwise yaw moment, with consequent oversteering and drift. The most evident effect of a μ drop, as can be clearly seen in Fig. 10, is a sudden decrease in the generated tire forces (from 6000 N to around 2000 N), with a consequent instability of the vehicle in cornering.

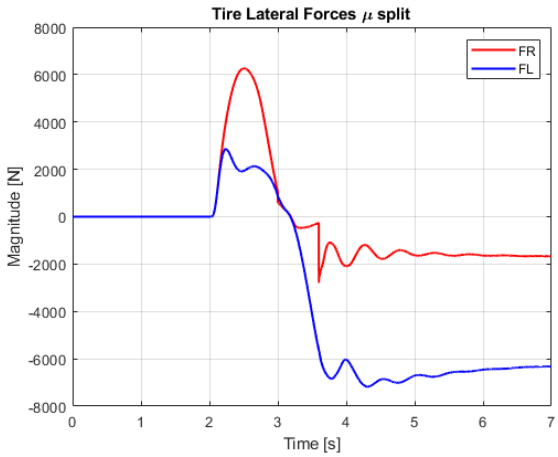

Fig. 10. Lateral forces on front left and front right wheel - Sine with dwell manoeuvre with μ-split

A phenomenon consequently related to this drop in the lateral force is the loss of directional control, that will eventually induce a drift of the vehicle in absence of control. As can be appreciated in Fig. 11, the skidding of the vehicle is evidently reduced with the implementation of a control strategy and, furthermore, the control appears to be optimized with the direct contribution of AFS, since with the additional control of the lateral velocity v_y the vehicle is able to achieve the largest distance from the obstacle in the critical point (1.07 s after the steering input) and the lowest cornering radius in closing the manoeuvre. Thus the vehicle performs best with Integrated Vehicle Control and provides higher control to the driver.

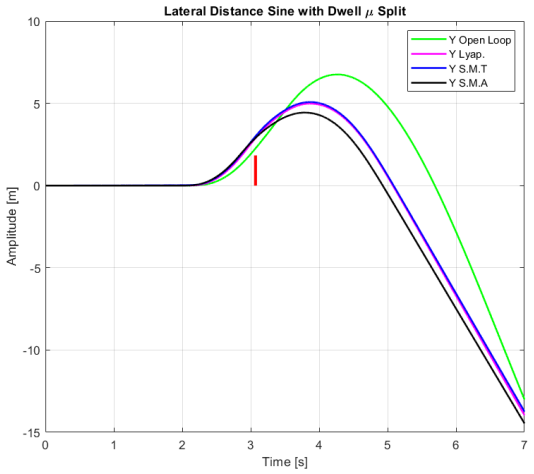

Fig. 11. Y displacement vs. time - Sine with dwell manoeuvre with mu-split

IV. Conclusions

ESC systems have gained popularity over the years, but however, still exhibit shortcomings. These can be seen in the number of fatal accident occurrences in systems equipped with ESC. To address this, principles in nonlinear control have been applied to come up with three strategies. The controller assessment illustrates the improvement in performance as the loop is closed. On assessment of the vehicle maneuverability, a number of manoeuvres were simulated. In the step steer input manoeuvre, the nonlinear state feedback controller performs better as one can see improvement in ride handling and comfort. However, other tests like skidpad and μ-split illustrate that the integrated controller comes out as the better solution. The reason is that, in addition to yaw rate control, lateral velocity is controlled using AFS.

References

[1] "Why do we need ESC?" [Online]. Available: https://www.newroads.ca/blog/need-electronic-stability-control-esc/

[2] https://crashstats.nhtsa.dot.gov//PublicationList/59, "Estimating lives saved by electronic stability control,2011-2015," March 2017.

[3] N. Hamzah, Y. M. Sam, H. Selamat, M. K. Aripin, and M. F. Ismail, "Vehicle stability enhancement based on second order sliding mode control," *IEEE International Conference on Control System, Computing and Engineering*, 2012.

[4] J. Guldner and V. Utkin, "The chattering problem in sliding mode systems."

[5] "Super-Twisting Sliding Mode Control." [Online]. Available: http://shodhganga.inflibnet.ac.in/bitstream/10603/42630/12/12_chapter%204.pdf

[6] Y. B. Shtessel, J. A. Moreno, F. Plestan, L. M. Fridman, and A. S. Poznyak, "Super-twisting adaptive sliding mode control: a lyapunov design," *49th IEEE Conference on Decision and Control*, 2010.

[7] J. J. Ley-Rosas, L. E. Gonzlez-Jimnez, A. G. Loukianov, and J. E. Ruiz-Duarte, "Robust observer-based sliding mode controller for vehicles with roll dynamics," *IEEE 55th Conference on Decision and Control (CDC)*, 2016.

[8] "Iso 4138 passenger cars steady-state circular driving behavior open-loop test methods," *ISO*, 2012.

Appendix
Nomenclature

TABLE I
Vehicle parameters used for simulating vehicle response

Symbol	Description	Value	Unit
M	total vehicle mass	1,900	$[kg]$
I_{xx}	Inertia along x-axis	700	$[kgm^2]$
I_{yy}	Inertia along y - axis	3,200	$[kgm^2]$
I_{zz}	Inertia along z-axis	3,500	$[kgm^2]$
r_{eff}	Effective Wheel Radius	0.3035	$[m]$
$r_{w,l}$	Wheel Loaded Radius	0.2866	$[m]$
m_{rim}	Rim mass	0.15	$[kg]$
m_{tire}	Tire mass	9.8	$[kg]$
$I_{xx,tire}$	Rim Inertia along x - axis	1	$[kgm^2]$
$I_{yy,tire}$	Rim Inertia along y - axis	1	$[kgm^2]$
l_f	Front Wheelbase	1.48	$[m]$
l_r	Rear Wheelbase	1.41	$[m]$
L	Total Wheelbase	2.89	$[m]$
h_{Bf}	Half of Front Trackwidth	0.5*1.56	$[m]$
h_{Br}	Half of Rear Trackwidth	0.5*1.58	$[m]$
h_{cg}	Height of CoG	0.54	$[m]$
h_r	Height of Rear Roll Center	0	$[m]$
h_f	Height of Front Roll Center	0	$[m]$
$m_{us,f}$	Front Axle mass	120	$[kg]$
$m_{us,r}$	Rear Axle mass	90	$[kg]$
Kz_f	Front Vertical Stiffness	52,000	$[N/m]$
Kz_r	Rear Vertical Stiffness	40,000	$[N/m]$
Dz_f	Front Vertical Damping Coefficient	3,000	$[Ns/m]$
Dz_r	Rear Vertical Damping Coefficient	3,000	$[Ns/m]$
$Kroll_f$	Front Roll Stiffness	130,000	$[N/rad]$
$Kroll_r$	Rear Roll Stiffness	40,000	$[N/rad]$
$Droll_f$	Front Roll Damping Coefficient	2,000	$[Ns/rad]$
$Droll_r$	Rear Roll Damping Coefficient	2,000	$[Ns/rad]$
i_s	Natural Steering Ratio	15.4	$[-]$
C_{α_f}	Front Cornering Stiffness	120,000	$[N/rad]$
C_{α_r}	Rear Cornering Stiffness	190,000	$[N/rad]$

TABLE II
Controllers' Tuning Parameters

Symbol	Value
A	1
B	1
K	250000
ϵ	1
W	10^6
σ_0	0.1
ρ	10^6
k_1	20
k_2	55
ω_1	3
ω_2	60
η_1	1
η_2	1
γ_1	1
γ_2	1
ϵ_1	0.001
ϵ_2	0.01